ELSEVIER

Contents lists available at ScienceDirect

Structural Safety

journal homepage: www.elsevier.com/locate/strusafe





Calibrating resistance factors of pile groups based on individual pile proof load tests

Yuting Zhang^a, Jinsong Huang^{a,*}, Jiawei Xie^a, Shan Huang^a, Yankun Wang^b

- a Surveving and Environmental Engineering. Priority Research Centre for Geotechnical Science and Engineering. The University of Newcastle. Callachan. NSW. Australia
- ^b School of Geosciences, Yangtze University, Wuhan, Hubei, China

ARTICLE INFO

Keywords:
Resistance factor
Pile group
Random finite difference method
Bayes' theorem

ABSTRACT

Pile load tests have been utilized to reduce the uncertainty of pile resistance, thus leading to a higher resistance factor used in the Load and Resistance Factor Design (LRFD). Previous studies have primarily focused on calibrating resistance factors for single piles based on load tests. This calibration hinges upon the resistance bias factor of single piles, defined as the ratio of measured resistance to predicted resistance. Due to the redundancy in the pile group system, it is conventionally assumed that if the individual piles within the group achieve a lower reliability index (e.g., 2.0-2.5), the pile group as a whole attains the target reliability index of 3. However, the approach is empirical as it does not consider system redundancy directly. Moreover, this empirical approach disregards the correlation between resistance bias factors of individual piles, which is inherently influenced by the spatial variability of soils. In this study, the random finite difference method (RFDM) is employed to evaluate the correlation between resistance bias factors of individual piles in spatially variable soils. The resultant correlation matrix is subsequentially employed in Bayes' theorem to update resistance bias factors using individual pile load test results and their corresponding test locations. The updated resistance bias factors are then used for the direct calibration of resistance factors for pile groups within the framework of LRFD. A pile group subject to vertical loading in undrained clays is adopted for illustration. Comparative analyses between the proposed approach and the empirical approach demonstrate that the latter tends to overestimate the resistance factor. Furthermore, the proposed approach enables the determination of optimal locations for conducting subsequent load tests based on previous test results.

1. Introduction

In the Load and Resistance Factor Design (LRFD), resistance factors are utilized to account for uncertainties associated with pile resistances. Nevertheless, the determination of resistance factors within design codes predominantly relies on engineering judgment, especially when load tests are performed [1]. For example, the Australian Standard for Piling-Design and Installation [2] outlines a formula to calculate the resistance factor, taking into account the overall risk rating, system redundancy, types of load tests and percentage of piles tested. However, the values assigned to parameters within the formula, such as the basic geotechnical strength reduction factor and the intrinsic test factor, which respectively represent the overall risk and types of load tests, primarily depend on expert judgment [3].

Several studies have been conducted to calibrate the resistance factor of single piles based on load test results [4–6]. Zhang and Tang [7]

evaluated the resistance factor of single piles based on load tests conducted to failure, and revealed that the resistance factor was increased by 30 % with only one load test conducted. Similar results were observed by Zhang, Li [8]. Zhang, Huang [1] proposed a probabilistic approach that integrates the First Order Reliability Method and the Bayesian approach to calibrate the resistance factor of H-piles using proof load tests. This approach also accommodates the consideration of site variabilities and design methods. Generally, the resistance factor of single piles is calibrated based on the statistics of the resistance bias factor, which is defined as the ratio of measured resistance to predicted resistance [4]. The statistics of resistance bias factors for single piles are typically derived from comprehensive load test databases, given the abundance of available data [9,10]. When load tests are conducted, test results are used to update the resistance bias factor, which is subsequentially adopted for recalibrating resistance factors of single piles. However, the extension of this approach to the realm of pile groups is

E-mail address: jinsong.huang@newcastle.edu.au (J. Huang).

^{*} Corresponding author.

not straightforward. Establishing the statistics of resistance bias factor for pile groups proves challenging due to the scarcity of field load tests conducted on the entire pile group. In practice, load tests are typically carried out on individual piles within a group, while load tests on the entire pile group are seldom performed owing to the complexity, high costs, time constraints, and limitations of the capacity of the loading equipment [11]. Consequently, there has been limited attention given to calibrating resistance factors of pile groups with load tests.

Currently, the determination of the resistance factor of pile groups mainly relies on empirical approaches. For instance, due to the redundancy in the pile group system, previous studies [12-20] recommended calibrating the resistance factor for individual piles within the group to achieve a reliability index of 2.0-2.5. This calibrated value is then assigned as the resistance factor for the pile group, aiming to attain the desired reliability index of 3. However, the approach is empirical as it does not consider system redundancy directly. Furthermore, this empirical approach disregards the correlation among resistance bias factors of individual piles, which is inherently influenced by the spatial variability of soils [21]. As a result, this empirical approach may yield unrealistic evaluations of resistance factors for pile groups. Alternatively, Oudah, El Naggar [22] and Alhashmi, Oudah [23] employed the system-based approach to calibrate resistance factors for pile groups. This approach utilized the binomial distribution to describe the probability of failure of the pile group if M or more out of N piles fail. Mrepresents the maximum number of failed piles that can occur without causing pile group failure and N denotes the total number of piles in the group. However, these studies failed to consider the correlation among individual piles. Moreover, the determination of the value of M presents a significant challenge due to the intricate failure mode exhibited by pile groups. Additionally, results obtained from individual pile load tests cannot be utilized for recalibrating resistance factors.

In this paper, a rigorous framework based on the random finite difference method (RFDM) and Bayes' theorem is proposed to calibrate resistance factors of pile groups with individual pile proof load tests. The proposed approach enables a direct calibration of resistance factors for pile groups, while also accounting for the correlation among resistance bias factors associated with individual piles. To achieve this, the RFDM is utilized to evaluate resistance bias factors of individual piles and their corresponding correlations in spatially variable soils. With individual pile load tests conducted, Bayes' theorem is employed to update the resistance bias factors using the test outcomes and their respective locations. Within the framework of LRFD, a limit state function of pile groups is formulated, and the updated resistance bias factors are integrated into this limit state function to directly calibrate resistance factors for pile groups. Notably, the proposed approach also facilitates the consideration of load test locations by integrating the correlation matrix of resistance bias factors into the Bayesian updating process. The paper is organized as follows: Section 2 introduces the methodology, elucidating the proposed approach in detail. Section 3 demonstrates the proposed approach using a 3 × 3 pile group subjected to vertical loadings in spatially variable soils. The results are presented and discussed in section 4, where the influence of various factors, such as the number of load tests, spatial variability of soils, and load test locations on resistance factors, is investigated. Moreover, this section highlights how the proposed approach is employed to identify the optimal location for conducting subsequent load tests based on previous test results. Finally, major findings are summarized in section 5.

2. Methodology

The proposed framework comprises three components: 1) the calibration of resistance factors for pile groups within LRFD, 2) the updating of the resistance bias factor based on individual pile load test results and their corresponding test locations, and 3) the determination of the resistance bias factors of individual piles and their corresponding correlations using RFDM. Further detailed explanations and discussions on

these three components are provided in the subsequent subsections.

2.1. Calibrating resistance factors of pile groups in LRFD

In LRFD, the resistance and load factors are employed to address the uncertainties related to resistance and loads, respectively. The design equation for pile groups is defined as the factored resistance is equal to or larger than the factored loads [24]:

$$\phi R_{gn} \ge \sum \gamma_i Q_{in}$$
 (1)

where ϕ is the resistance factor, R_{gn} is the nominal pile group resistance. γ_i is the load factor, Q_{in} is the nominal load.

For the purpose of calibration, Eq. (1) is of interest when the factored resistance and factored loads are equal. In this paper, only dead and live loads are considered, leading to a simplification of the design equation as follows:

$$\phi R_{gn} = \gamma_D Q_{Dn} + \gamma_L Q_{Ln} \tag{2}$$

where γ_D and γ_L are the dead load factor and live load factor, respectively. Q_{Dn} and Q_{Ln} are the nominal dead load and nominal live load, respectively.

In Eq. (2), load factors are adopted from AASHTO [24] and are assigned specific values corresponding to different limit states. For example, $\gamma_D=1.25$ and $\gamma_L=1.75$ if the Strength I limit state is considered, while $\gamma_D = \gamma_L = 1.0$ if the Service I limit state is considered. Q_{Dn} and Q_{Ln} represent the nominal loads transferred from the superstructure to the substructure, and these values are obtained through structural analysis. For the pile group resistance, the concept of group efficiency, η , is adopted, which has been traditionally employed in engineering practice [25]. η is defined as the ratio of the pile group resistance, R_g , to the summation of the individual pile resistance, $\sum_{i=1}^{N} R_i$, [26]. Therefore, for a pile group containing N piles, R_g is calculated as: $R_g = \eta \sum_{i=1}^{N} R_i$. It is worth noting that the assessment of η in this paper involves the consideration of spatially variable soils, as described in section 2.3, in contrast to previous studies that predominantly assumed uniform soil properties [27]. Given the consideration of soil spatial variability herein, η should be treated as a random variable instead of a constant value, as it is inherently influenced by the soil properties [28]. It is assumed that the mean group efficiency, η_n , is used to derive the nominal pile group resistance. Therefore, R_{gn} is determined as follows:

$$R_{gn} = \eta_n \sum_{i=1}^{N} R_{in} \tag{3}$$

where R_{in} is the nominal resistance of the *i*th pile, defined as the mean pile resistance obtained by RFEM. Thus, the nominal resistances of individual piles are identical, $R_n = R_{1n} = \dots = R_{Nn}$.

The limit state function, *g*, is defined as the pile group resistance equals the sum of loads transferred from the superstructure:

$$g = R_g - Q_D - Q_L = \eta \sum_{i=1}^{N} R_i - Q_D - Q_L = 0$$
 (4)

where R, Q_D and Q_L are the measured resistance, dead load and live load, respectively.

In engineering practice, empirical design methods are commonly employed to estimate resistance and loads by utilizing simplified models and assumed model parameters. This often leads to predicted values that deviate from actual measurements. Furthermore, the idealization of soil layers, the assignment of constant soil properties within each layer, and the uncertainty introduced during the evaluation of soil properties via bivariate correlations can exacerbate the discrepancies between predicted and measured pile resistances. To address these discrepancies in resistance, dead load, and live load, three random variables are intro-

duced: the resistance bias factor, λ_R , dead load bias factor, λ_D , and live load bias factor, λ_L . For a pile group contains N piles, λ_R is a vector that contains λ_{1R} , ..., λ_{NR} , $\lambda_R = (\lambda_{1R}$, ..., λ_{NR}). There bias factors are defined as the ratio of the measured value to the predicted one. Additionally, it is assumed that the predicted value is employed as the nominal value in designs. Therefore, the relationship between the nominal values and the corresponding measured values is specified by the following transformations [17]:

$$R_i = \lambda_{iR} R_n \quad Q_D = \lambda_D Q_{Dn} \quad Q_L = \lambda_L Q_{Ln} \tag{5}$$

By substituting Eqs. (2), (3) and (5) into Eq. (4) and introducing the ratio of dead to live load, denoted as $\kappa = Q_{Dn}/Q_{Ln}$, the limit state function of pile groups is derived as follows:

$$g = \frac{\lambda_{\eta}}{N\phi} \times \sum_{i=1}^{N} \lambda_{iR} \times (\gamma_{D}\kappa + \gamma_{L}) - (\lambda_{D}\kappa + \lambda_{L}) = 0$$
 (6)

where λ_{η} is defined as the ratio of the group efficiency and the mean of group efficiency, $\lambda_{\eta}=\eta/\eta_{n}$.

In Eq. (6), κ exhibits variability across diverse superstructures, typically spanning values within the range of 2 to 5 [29]. Nevertheless, it has been demonstrated that κ exerts a negligible impact on resistance factors [12]. As aforementioned, that λ_n is defined as the group efficiency normalized by its mean. In the presence of spatially variable soils, the group efficiency itself is considered a random variable, thereby making λ_n a random variable as well. The RFEM is employed to determine λ_{η} , as explained in section 2.3. For the purpose of foundation design, λ_D and λ_L are assumed to follow lognormal distributions, and their mean values (i.e., μ_{λ_D} and μ_{λ_L}) and standard deviations (i.e., σ_{λ_D} and σ_{λ_L}) are adopted from Paikowsky [13]. Consequently, the main task of calibrating resistance factors is to determine the distribution and corresponding statistics of $\lambda_{iR},\ i=1\ ,\ 2\ ,\ \ldots\ ,\ N.$ The process of determining $\lambda_{R} = (\lambda_{1R} \ , \ \dots \ , \ \lambda_{NR})$ using the RFDM is outlined in section 2.3. The obtained results of λ_R serve as prior information for calibrating the resistance factor. Furthermore, if load tests are conducted on individual piles within the group to verify their resistance, λ_R is updated by load test results, leading to adjustments in the resistance factor to attain the target reliability index. The framework for updating λ_R using load test results is presented in section 2.2.

In order to calibrate resistance factors based on Eq. (6), a predetermined target reliability index of the pile group, β_{GT} , is required. Extensive research efforts have been undertaken to explore the reliability indices of foundations. Meyerhof [30] reported reliability indices ranging from 3.0 to 3.6 for foundations, while Tang, Woodford [31] revealed reliability indices in the range of 1.4 to 3.0 for offshore piles. In the realm of pile foundation designs, a target reliability index of 3 is commonly employed [21,32], and it is also adopted in this study. Consequently, the resistance factor of pile groups is calibrated to attain a reliability index of 3 based on the statistics of λ_{η} , λ_{R} , λ_{D} , and λ_{L} .

2.2. Updating resistance bias factors with load test results

$$f'(\lambda_R) \propto \frac{1}{\prod_{i=1}^{N} \lambda_{iR}} \times \exp\left(-\frac{1}{2} \left(\frac{\ln \lambda_{iR} - \mu'_{\ln \lambda_R}}{\sigma'_{\ln \lambda_R}}\right)^{\mathrm{T}} C^{-1} \left(\frac{\ln \lambda_{iR} - \mu'_{\ln \lambda_R}}{\sigma'_{\ln \lambda_R}}\right)\right)$$
(7)

where $\mu'_{\mathrm{ln}\lambda_R}$ and $\sigma'_{\mathrm{ln}\lambda_R}$ are the mean and standard deviation of $\mathrm{ln}\lambda_{iR}$, respectively. $\sigma'_{\mathrm{ln}\lambda_R} = \sqrt{\ln\left(1+\left(\sigma'_{\lambda_R}/\mu'_{\lambda_R}\right)^2\right)}$ and $\mu'_{\mathrm{ln}\lambda_R} = \mathrm{ln}\mu'_{\lambda_R} - 1/2\sigma'^2_{\mathrm{ln}\lambda_R}$.

C is a N by N correlation matrix with the diagonal terms equal to unity and the off-diagonal terms equal to r_{ij} .

With the completion of proof load tests on individual piles, the test outcomes are used to update the resistance bias factor. The test load is denoted as T, and $\lambda_T = T/R_n$. It is important to acknowledge that the load test measurements are subject to inherent errors and uncertainties. To account for these factors, the measurement error, denoted as ε , is assumed to follow a normal distribution with a mean of μ_s and a standard deviation of σ_{ε} . Therefore, the actual load applied to tested piles is $T-\varepsilon$. However, it should be noted that limited guidance is available on how to quantify the magnitude of the measurement error. Hence, further research efforts are necessary to address this crucial issue. For simplification, it is assumed that $\mu_{\varepsilon} = 0$ and σ_{ε} exhibits a proportional relationship with the corresponding measurements, denoted as $\sigma_{\varepsilon} = \alpha T$. The value of α is contingent upon the specific load test techniques employed as well as the methodologies applied for the interpolation of test results. Under these assumptions, the likelihood function of pile i passes the proof load test is derived as follows:

$$\begin{split} L(\lambda_{iR}|R_{i} > T - \varepsilon) \propto & P(R_{i} > T - \varepsilon|\lambda_{iR}) = P(\varepsilon > T - R_{i}|\lambda_{iR}) = 1 - P(\varepsilon \le T - R_{i}|\lambda_{iR}) \\ &= 1 - P\left(\frac{\varepsilon - \mu_{\varepsilon}}{\sigma_{\varepsilon}} \le \frac{(T - R_{i}) - \mu_{\varepsilon}}{\sigma_{\varepsilon}} \Big| \lambda_{iR}\right) \\ &= 1 - P\left(\frac{\varepsilon - \mu_{\varepsilon}}{\sigma_{\varepsilon}} \le \frac{(T/R_{n} - R_{i}/R_{n}) - \mu_{\varepsilon}/R_{n}}{\sigma_{\varepsilon}/R_{n}} \Big| \lambda_{iR}\right) \\ &= 1 - P\left(\frac{\varepsilon - \mu_{\varepsilon}}{\sigma_{\varepsilon}} \le \frac{\lambda_{T} - \lambda_{iR}}{\alpha} \Big| \lambda_{iR}\right) = 1 - \Phi\left(\frac{\lambda_{T} - \lambda_{iR}}{\alpha}\right) \\ &= \Phi\left(\frac{\lambda_{iR} - \lambda_{T}}{\alpha}\right) \end{split}$$

$$(8)$$

where Φ is the cumulative distribution function of the standard normal distribution.

The individual piles within the group are sequentially numbered as $1, 2, \ldots, N$. Considering the proof load test performed on a total of n piles, where m piles fail, the number associated with the failed pile is denoted as $\boldsymbol{f} = (f_1, \quad f_2, \cdots, f_m)$, and the number associated with the passed pile is denoted as $\boldsymbol{p} = (p_1, \quad p_2, \cdots, p_{n-m})$. Thus, the observations are: $R_{f_1} < T - \varepsilon, \quad R_{f_2} < T - \varepsilon, \ldots, \quad R_{f_m} < T - \varepsilon, \quad \text{and} \quad R_{p_1} \geq T - \varepsilon, \quad R_{p_2} \geq T - \varepsilon, \ldots, \quad R_{p_{n-m}} \geq T - \varepsilon$. The likelihood function for m tests fail among n tests is expressed as follows:

$$L(\lambda_R|\text{Observations}) \propto \prod_{i=f_1}^{f_m} \left(1 - \Phi\left(\frac{\lambda_{iR} - \lambda_T}{\alpha}\right)\right) \prod_{i=p_1}^{p_{n-m}} \Phi\left(\frac{\lambda_{iR} - \lambda_T}{\alpha}\right)$$
(9)

The posterior distribution of $\lambda_R = (\lambda_{1R} \ , \ \dots \ , \ \lambda_{NR})$ is obtained by employing Bayes' theorem [33]:

 $f''(\lambda_R|\text{Observations}) \propto L(\lambda_R|\text{Observations}) f'(\lambda_R)$

$$\propto \prod_{i=f_1}^{f_m} \left(1 - \Phi\left(\frac{\lambda_{iR} - \lambda_T}{\alpha}\right) \right) \prod_{i=p_1}^{p_{n-m}} \Phi\left(\frac{\lambda_{iR} - \lambda_T}{\alpha}\right)$$

$$\frac{1}{\prod_{i=1}^{N} \lambda_{iR}} exp\left(-\frac{1}{2} \left(\frac{\ln \lambda_{iR} - \mu'_{\ln \lambda_R}}{\sigma'_{\ln \lambda_R}}\right)^{\mathrm{T}} C^{-1} \left(\frac{\ln \lambda_{iR} - \mu'_{\ln \lambda_R}}{\sigma'_{\ln \lambda_R}}\right) \right)$$

$$(10)$$

It is noted that the Eq. (10) are complex and impossible to solve analytically. Thus, the Markov chain Monte Carlo [34] is adopted to sample the posterior distribution.

2.3. Determining λ_R , C, and λ_n by RFDM

The RFDM, which integrates the FD analysis with random field theory in conjunction with Monte Carlo simulation (MCS) is employed to evaluate λ_R , C, and λ_n in spatially variable soils. In the context of pile foundations situated in undrained clay, the pile resistance is predominantly influenced by the undrained shear strength, c_u , [35,36]. Therefore, only c_u is modelled as stationary random fields in this paper, while other parameters (e.g., shear modulus) are treated as constant. The random field theory is employed to generate a 3D spatially distributed undrained shear strength, c_u , based on specified statistical parameters, including mean, μ_{c_u} , coefficient of variation, COV_{c_u} , and spatial correlation length, θ . The FD software FLAC3D [37] is utilized to compute the resistances of both the pile group and individual piles in spatially variable soils. For each set of statistical parameters of c_u , MCS is performed. These involve 100 realizations of the undrained shear strength random field and the subsequent FD analysis of pile resistances. Statistical analyses demonstrate that the mean and standard deviation of desired parameters (e.g., λ_R and λ_η) stabilize after 70 simulations, supporting the sufficiency of 100 simulations.

In each simulation, the individual pile resistances are determined. Initially, a single pile FD model is constructed. Subsequently, a small incremental displacement is applied to the pile top at each step, while the vertical load on the pile is obtained using the embedded function 'force'. The load-displacement curve of the pile is then generated after executing a substantial number of steps (e.g., 50000). The pile resistance is determined based on the load-displacement curve and the prescribed failure criterion (e.g., ISSMFE criterion [38]). It is worth noting that the pile resistance defined by different failure criteria can vary significantly [39]. For demonstration, the ISSMFE criterion [38] is adopted in this paper, which corresponds to the displacement of piles is 10 % of the pile diameter. The mean and standard deviation of the individual pile resistances are then calculated based on the outcomes of 100 simulations. It is assumed that the resistance obtained from a rigorous 3D FD analysis is unbiased and equivalent to the measured resistance when the soil parameters are known precisely, and the variability in λ_{iR} , primarily arises from the spatial variability in soil strength. As a result, λ_{iR} is computed as the ratio of the individual pile resistance obtained by FD analysis and nominal resistance, where the nominal resistance is obtained by FD analysis based on the mean soil strength. The mean and standard deviation of λ_{iR} obtained through the RFDM serve as prior information (i.e., μ'_{λ_R} , σ'_{λ_R}), as elaborated in section 2.2.

After completing the RFDM analysis, 100 sets of $\lambda_R = (\lambda_{1R} \ , \ \dots \ , \lambda_{NR})$ are obtained. Consequently, correlation analyses are performed to establish the correlation matrix, C.

Furthermore, the pile group resistance is obtained in each simulation. For the purpose of simplification, a rigid pile cap is assumed. Moreover, only vertical displacement is permitted when subjected to vertical loads, while the rotation of the cap is not considered. These assumptions restrict all piles to undergo equal head displacements under vertical loads. This approach aligns with the simplifications commonly employed in previous studies concerning rigid footings and pile group foundations [40,41] situated in spatially variable soils and subjected to vertical loads. The consideration of cap rotation may lead to complex failure modes due to induced bending moments and shear forces in individual piles [42,43], which falls beyond the scope of this paper. In the FD analysis, a pile group FD model is initially constructed. Subsequently, the same displacement is applied to the top of individual piles at each step, while the vertical loads on individual piles are obtained using the embedded function 'force'. The load-displacement curves of individual piles within the group are generated after executing a substantial number of steps (e.g., 50000). The total load acting on the pile group is calculated as the sum of the loads on individual piles [44], and the displacement of the pile group is equivalent to that of individual piles. Consequently, a load-displacement curve for the pile group is obtained,

and the same failure criterion utilized for individual piles is employed to determine the pile group resistance. η is computed by dividing the pile group resistance by the sum of individual pile resistances. Subsequently, the mean and standard deviation of η are determined based on 100 values of η . As for λ_{η} , it is computed as the ratio of η and its mean value.

2.4. Procedure of the proposed approach

The procedure of the proposed approach is summarized as follows: Step 1: Generate stationary random fields of c_u based on specified statistical parameters. Map the value of c_u to the corresponding soil element in the FD model.

Step 2: Compute the resistances of both the pile group and individual piles using the same soil property.

Step 3: Determine λ_{η} and C, and prior distribution of λ_{R} , as described in section 2.3.

Step 4: Evaluate the posterior distribution of λ_R by utilizing the number of tests, test outcomes and their respective locations. This evaluation is performed following the procedure outlined in section 2.2.

Step 5: Generate N_T (i.e., ten million) sets of samples for λ_D , λ_L , and λ_η , while the samples generated in step 4 are utilized for λ_R .

Step 6: Steps 6–9 describe the optimization of ϕ based on the Bisection method. To guarantee convergence, a broader initial range for ϕ , specifically [0, 2], has been selected. The midpoint of this range, 1, is then adopted as the trail ϕ for evaluating the limit state function, g, (i.e., Eq. (6)) for each set of samples.

Step 7: Count the number of cases where $g \le 0$, N_f . Calculate the probability of failure, $p_f = N_f/N_T$.

Step 8: Calculate the reliability index, $\beta = \Phi^{-1}(1 - p_f)$, where Φ^{-1} is the inverse cumulative distribution function of the standard normal distribution.

Step 9: Compare β with the target reliability index, β_{GT} . If $\beta > \beta_{GT}$, it suggests that the trial ϕ is conservatively low, and hence, the range is adjusted to [1, 2] with a new trail ϕ of 1.5. Conversely, if $\beta < \beta_{GT}$, it indicates that the trial ϕ is overly high, necessitating a revision of the range to [0, 1] with a new trail ϕ of 0.5. This iterative process is continued until $|\beta - \beta_{GT}| \leq 0.01$.

3. Example

To demonstrate the proposed approach, a 3×3 pile group under vertical loading in undrained clay is employed. The arrangement of the pile group is shown in Fig. 1 (a), where individual piles are sequentially numbered from 1 to 9. Additionally, Fig. 1 (b) depicts the representative FD model of the pile group in spatially variable soils. The soil medium is modelled as a cuboid with dimensions of $30\times30\times20$ m. To facilitate the generation of a random field and the mapping of soil properties to individual elements, the soil medium is discretized into 8-noded cubic elements with a uniform side length of 1 m. The pile-element represents the pile as a linear structural element with interface properties, eliminating the need for explicit modelling of the physical geometry of piles [27,45]. Given that the analysis is focused on free-standing pile groups, there is no necessity to include a pile cap in the FD model. The pile geometry parameters, as well as the relevant pile and soil properties employed in FD models, are summarized in Table 1.

The undrained shear strength, c_u , is modelled as a lognormal distribution to prevent negative values for the soil property [46]. The spatial correlation length, θ , is nondimensionalized by the embedded length (l), and the normalized spatial correlation length is expressed as $\Theta = \theta/l$. The generation of a 3D stationary random field of c_u is accomplished using the randomization method described in Heße, Prykhodko [47], based on $\mu_{c_u} = 20$ kPa, while COV_{c_u} and Θ vary within the ranges of 20 to 100 %, and 0.15 to 5, respectively. This study adopts the isotropic spatial correlation length for demonstration purposes, motivated by several considerations: 1) the application of isotropic spatial correlation lengths

Y. Zhang et al. Structural Safety 111 (2024) 102517

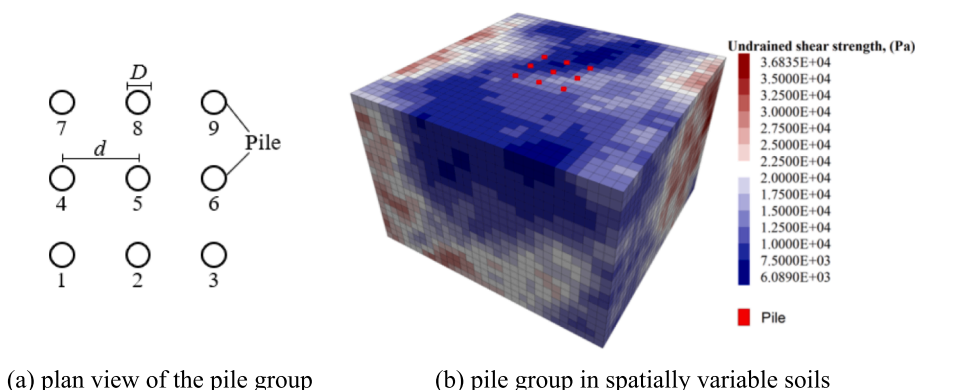


Fig. 1. The FD model of pile groups. (a) plan view of the pile group (b) pile group in spatially variable soils.

Table 1The properties of pile and soil in the FD model.

Pile	Value
Length,L	10.5 m
Embedded length,l	10 m
Diameter,D	1.0 m
Spacing,d	3.0 m
Elastic modulus, E_P	$2.2 \times 10^7 \text{ kPa}$
Poisson ratio	0.3
Soil	Value
Mean of undrained shear strength, μ_{c_u}	20 kPa
Coefficient of variation of undrained shear	20 %, 30 %, 50 %, and 100
strength, COV_{c_u}	%
Normalized spatial correlation length,⊖	0.15, 0.5, 1, 2, and 5
Shear modulus,G	$1.3 imes 10^3 \mathrm{kPa}$
Bulk modulus,K	$6.0 imes 10^3 ext{ kPa}$

remains prevalent in the most recent research regarding the reliability analysis of piles [48–50]; 2) illustrating the impact of load test locations becomes challenging with the use of a large horizontal correlation length. Nonetheless, it should be noted that the proposed approach can be utilized to consider anisotropic spatial correlation lengths.

The load factors are adopted from AASHTO [24] with $\gamma_D=1.25$ and $\gamma_L=1.75$. The statistics of load bias factors are obtained from Paikowsky [13] with $\mu_{\lambda_D}=1.05$, $\mu_{\lambda_L}=1.15$, $\sigma_{\lambda_D}=0.105$, and $\sigma_{\lambda_L}=0.23$. The ratio of dead to live load, κ , is assumed to be 2, while the target reliability index, β_{GT} , is set to 3. In proof load tests, it is assumed that the test load corresponds to the nominal resistance of individual piles, $T=R_n$. The standard deviation of measurement error is assumed to be 0.1T, denoted as $\sigma_{\varepsilon}=0.1T$.

4. Results

4.1. Effect of the number of tests and test outcomes

This subsection aims to investigate the impact of the number of tests, n, and the number of failed tests, m, on the resistance factor, ϕ . The resistance factors are obtained using both the proposed approach and the empirical approach to facilitate a comprehensive comparison. The tests are assumed to be performed in accordance with the sequential numbering of individual piles, and it is further assumed that the negative tests (i.e., tested piles fail) are observed prior to the positive tests (i.e., tested piles pass). For instance, n=4 and m=2 denotes that pile 1, pile 2, pile 3 and pile 4 are tested sequentially, where pile 1 and pile 2 fail while pile 3 and pile 4 pass. It should be noted that, while different test outcome combinations influence the absolute values of resistance factors, they do not alter the overall trend of resistance factors nor the comparative analysis between the proposed and empirical approaches. Consequently, for the purpose of clarity in this subsection, a single

permutation (i.e., negative tests are observed prior to the positive tests) has been selected for demonstration, with a detailed investigation of various combinations for specified values of n and m to be conducted in sections 4.4 and 4.5.

Fig. 2 illustrates the variation of resistance factors with respect to *n* and m, for $\Theta = 2$ and $COV_{c_n} = 50\%$. As expected, for a fixed value of n, ϕ decreases as m increases. Fig. 2 reveals that ϕ obtained using the empirical approach are generally higher than those generated by the proposed approach, indicating that the empirical approach may lead to unconservative designs. This discrepancy can be attributed to two primary factors. Firstly, the empirical approach relies on the subjective selection of the target reliability index for individual piles, β_{ST} . A lower value of β_{ST} yields a higher ϕ , whereas a higher value of β_{ST} corresponds to a lower ϕ . In this example, a commonly accepted value of $\beta_{ST}=2.33$ is utilized, which leads to an overestimated ϕ . Secondly, the empirical approach disregards the spatial variability of soils, resulting in the assumption of perfect correlation among individual piles. With load tests performed, the variation of the resistance bias factors for untested piles is reduced to the same value as tested piles. In contrast, the proposed approach considers the spatial variability of soil strength and the relative positions of individual piles, leading to imperfect correlation among the piles. As a result, if the untested piles are uncorrelated with the tested piles, the variation of the resistance bias factors for untested piles remains unchanged, resulting in a lower ϕ that can be used for the pile group to achieve the target reliability.

In Fig. 2, points A, B and C are obtained by the empirical approach,

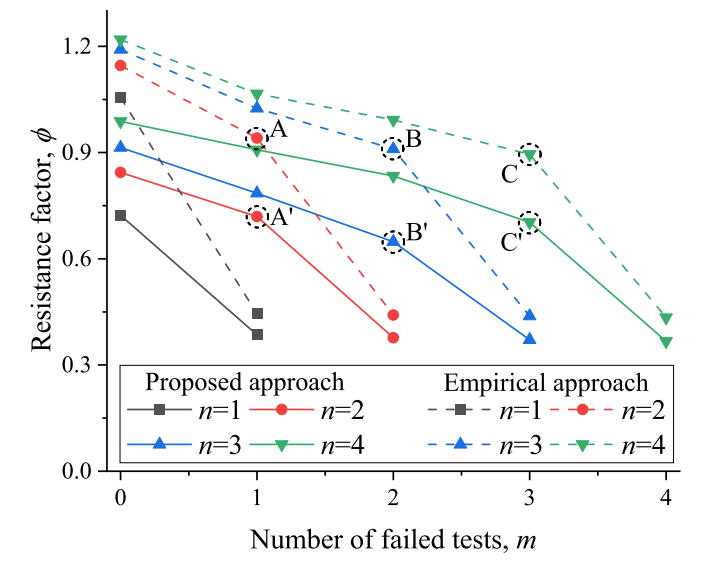


Fig. 2. Resistance factors for different *n* and *m*, with $\Theta = 2$ and $COV_{c_n} = 50\%$.

Y. Zhang et al. Structural Safety 111 (2024) 102517

denoting that one among two tests fails, two among three tests fail and three among four tests fail, respectively, while points A', B' and C' are obtained by the proposed approach. It is worth noting that, in the empirical approach, ϕ associated with A, B and C gradually decreases owing to the increase in m. In contrast, ϕ corresponding to A', B' and C' does not exhibit a monotonic trend due to consideration of load test locations. A' indicates pile 1 fails and pile 2 passes, B' signifies pile 1 and pile 2 fail while pile 3 passes, and C' represents pile 1, pile 2 and pile 3 fail while pile 4 passes. The higher ϕ associated with point B' compared to that of point C' suggests that pile 4 (i.e., the edge pile) provides more significant information regarding the reliability of pile groups than pile 3 (i.e., the corner pile), which aligns with common engineering practice. The observations reveal a limitation of the empirical approach in failing to account for the influence of load test locations, unlike the proposed approach. To investigate the significance of load test locations and their impact on ϕ , a comprehensive analysis is provided in sections 4.4 and

4.2. Effect of the spatial correlation length

The effect of Θ on resistance factors for n=4 and $COV_{c_n}=50\%$ is illustrated in Fig. 3. Once again, the load tests are performed in accordance with the sequential numbering of individual piles, with the negative tests being observed prior to the positive tests. Fig. 3 shows that, irrespective of the value of m, ϕ initially decreases and subsequently increases as Θ increases from 0.15 to 5. For example, when m=2, ϕ decreases from 0.95 to 0.82 as Θ increases from 0.15 to 1, and then slightly increases to 0.84 as Θ further increases to 5. In all cases depicted in Fig. 3, a worst-case spatial correlation length of $\Theta = 1$ is observed where ϕ attains its minimum value. In practice, the worst-case spatial correlation length could serve conservative design purposes, particularly in situations where data limitations impede the accurate estimation of Θ. It is imperative to highlight that ϕ exhibits relatively higher values when $\Theta = 0.15$. Under this circumstance, the correlation coefficient of the resistance bias factor among individual piles remains lower than 0.25, indicating that the failure of certain piles has a limited impact on untested ones. In this context, the presence of weaker piles can be compensated by stronger ones, thereby enhancing the overall reliability of the entire pile group. Consequently, the rationale behind adopting a higher ϕ becomes substantially justifiable.

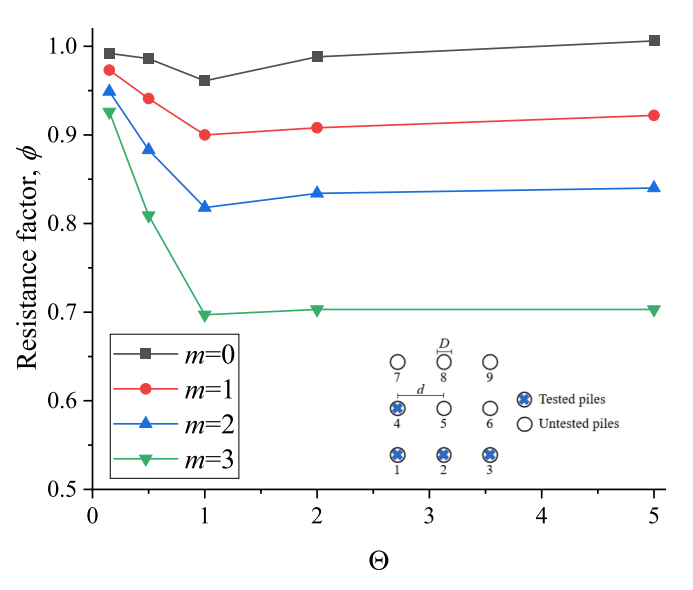


Fig. 3. Resistance factors for different Θ and m, with n = 4 and $COV_{c_n} = 50\%$.

4.3. Effect of the coefficient of variation

The influence of COV_{c_u} on resistance factors for n=4 and $\Theta=5$ is presented in Fig. 4. Similar to the assumption in sections 4.1 and 4.2, the load tests are performed following the sequential numbering of individual piles, with the negative tests being observed before the positive tests. Fig. 4 demonstrates that, for a fixed value of m, ϕ exhibits an increasing trend as COV_{c_u} decreases. For instance, when m=2, ϕ shows an increase from 0.71 to 0.90 as COV_{c_u} decreases from 100 % to 20 %. This phenomenon is attributed to the fact that pile resistance is primarily influenced by c_u , and a high variability in c_u induces a greater variability in pile resistance, leading to a reduced reliability of the pile group. Therefore, a lower ϕ is necessary to attain the target reliability. Additionally, Fig. 4 reveals a decreasing trend in ϕ as m increases. Specifically, when $COV_{c_u}=100\%$, ϕ decreases from 0.89 to 0.57 as m increases from zero to three.

4.4. Effect of load test locations

The purpose of this subsection is to investigate the impact of load test locations on resistance factors. It is noteworthy that there exist various configurations of load test locations for a given number of tests and their respective outcomes. For instance, when one load test is performed, three distinct options arise irrespective of the test result: the corner pile (i.e., pile 1, pile 3, pile 7, and pile 9), the edge pile (i.e., pile 2, pile 4, pile 6, and pile 8), or the centre pile (i.e., pile 5). In contrast, with two load tests conducted, the potential combinations extend to eight permutations if both tests yield positive results, and twelve permutations if the first test yields a negative result followed by a positive result in the second test. The number of potential combinations significantly increases with the number of tests. Therefore, for illustration, this subsection adopts the scenario involving two load tests, both yielding positive results.

The change of ϕ with respect to the load test locations and Θ , with n=2, m=0 and $COV_{c_u}=50\%$ is shown in Fig. 5. The notation 'Piles 1+2' signifies that the load tests are sequentially conducted on pile 1 and pile 2. It is observed from Fig. 5 that the impact of load test locations on ϕ is negligible when $\Theta=0.15$. In this case, the tested piles have no influence on the untested ones, and the updated ϕ is solely affected by the number of tests conducted and their corresponding outcomes. It is speculated that in the extreme case, where $\Theta \rightarrow \infty$, the individual piles are perfectly correlated, the test locations have a negligible impact on ϕ . However, for intermediate spatial correlation lengths, ϕ exhibits

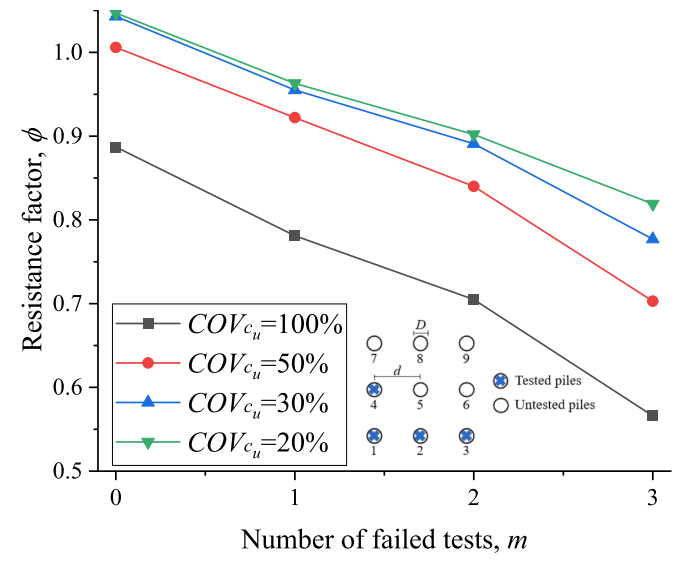


Fig. 4. Resistance factors for different COV_{c_n} and m, with n=4 and $\Theta=5$.

Y. Zhang et al. Structural Safety 111 (2024) 102517

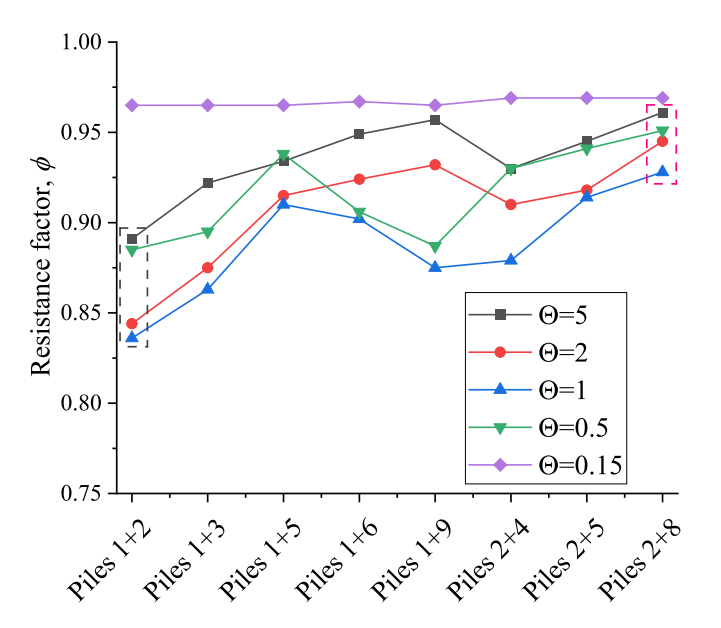


Fig. 5. Resistance factors for different test locations and Θ , with $COV_{c_u} = 50\%$

dependence on the test locations, as depicted in Fig. 5. For example, ϕ ranges from 0.84 to 0.95 for $\Theta=2$. Notably, the highest ϕ is obtained when pile 2 and pile 8 are tested, while the lowest ϕ is obtained when pile 1 and pile 2 are tested. These results are also reflected in Fig. 6, which presents ϕ for different test locations and COV_{c_u} , with n=2, m=0 and $\Theta=2$. Additionally, Fig. 6 indicates that the trend of ϕ with respect to load test locations remains consistent across different values of COV_{c_u} . Specifically, when the first load test is conducted on pile 1, ϕ progressively increases as subsequent load tests are performed on pile 2, pile 3, pile 5, pile 6, and pile 9. Conversely, if the first load test is conducted on pile 2, ϕ gradually increases with subsequent tests conducted on pile 4, pile 5, and pile 8.

4.5. Optimal test locations based on previous test results

This subsection aims to illustrate the application of the proposed approach in determining optimal locations for conducting subsequent load tests based on acquired test results. Fig. 7 depicts ϕ obtained from

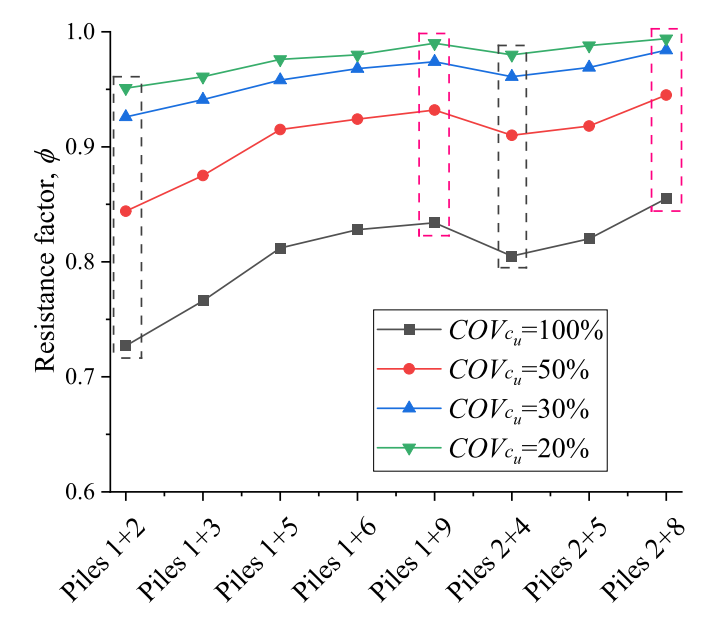


Fig. 6. Resistance factors for different test locations and COV_{c_0} , with $\Theta = 2$.

various load test configurations, with $\Theta=2$ and $COV_{c_u}=50\%$. The initial resistance factor corresponds to the scenario where no tests are conducted. It is calibrated by utilizing the prior distribution of resistance bias factors. The notation 'P' denotes that the tested piles pass the proof test, while 'F' indicates that the tested piles fail. Owing to the symmetric configuration of the pile group, three distinct scenarios emerge for conducting the first test, namely pile 1, pile 2, or pile 5. Subsequently, ϕ is calibrated based on the specific test location and the corresponding test result, according to the steps described in section 2.4. Depending on the first load test, various choices emerge for determining the second test location. Consequently, ϕ is recalibrated based on the selected location and the second load test result. All load test configurations and their corresponding ϕ are presented in Fig. 7, which can be readily applied in engineering practice.

In Fig. 7, when one load test is conducted, the load test on pile 5 with a positive result yields the highest ϕ , indicating that pile 5 is the best location to conduct the first test. However, it is also noteworthy that when two load tests are conducted, the highest ϕ is obtained when pile 2 and pile 8 yield positive results (i.e., route 1). Thus, pile 2 emerges as another viable choice for the first test. The observation indicates that pile 2 and pile 5 are viable choices for conducting the first load test if multiple tests are to be performed.

Results shown in Fig. 7 can be utilized to determine the optimal location for conducting subsequent load tests based on obtained test results. For example, if the first load test is performed on pile 2 with a positive outcome, it is advisable to conduct the second load test on pile 8 to achieve the highest ϕ (i.e., route 1). Conversely, if the first load test on pile 2 yields a negative result, the optimal location for the subsequent load test is identified as pile 5 (i.e., route 2). In the case where the first load test is performed on pile 5, it is recommended to conduct the second load test on pile 2, regardless of the first test result (i.e., route 3 and route 4). These findings contribute valuable instructions for designing load test schemes and offer practical guidance for engineering practices. It should be noted that the illustrative example is limited to a scenario involving a single soil layer with spatially variable properties. The impact of soil stratification on the optimal testing locations remains an area for future investigation.

5. Conclusions

This paper proposes a rigorous framework to directly calibrate resistance factors of pile groups with individual pile proof load tests. The impact of the number of tests, load outcomes, spatial variability of soils and test locations on resistance factors can be considered. A 3 \times 3 pile group is adopted to demonstrate the proposed approach. The following conclusions are made from this study:

- 1. A comparative analysis is performed to evaluate the resistance factors obtained using the proposed approach and the empirical approach. The findings demonstrate that the empirical approach, which involves the subjective selection of the target reliability index for individual piles and disregards the spatial variability of soils, may lead to unconservative designs. In contrast, the proposed approach overcomes these limitations by incorporating the RFDM into the calibration process.
- 2. There is a worst-case spatial correlation length where the resistance factor calibrated based on load test results is minimal. This finding has significant implications for conservative designs, particularly when the evaluation of the spatial correlation length is constrained by limited site investigation data.
- 3. At intermediate spatial correlation lengths, the resistance factors are significantly influenced by load test locations. In the case of one load test, the highest resistance factor is obtained when the test is conducted on the centre pile and yields a positive result. In the case of two load tests, the highest resistance factor is attained when the tests are performed on the opposite edge piles and yield positive results.

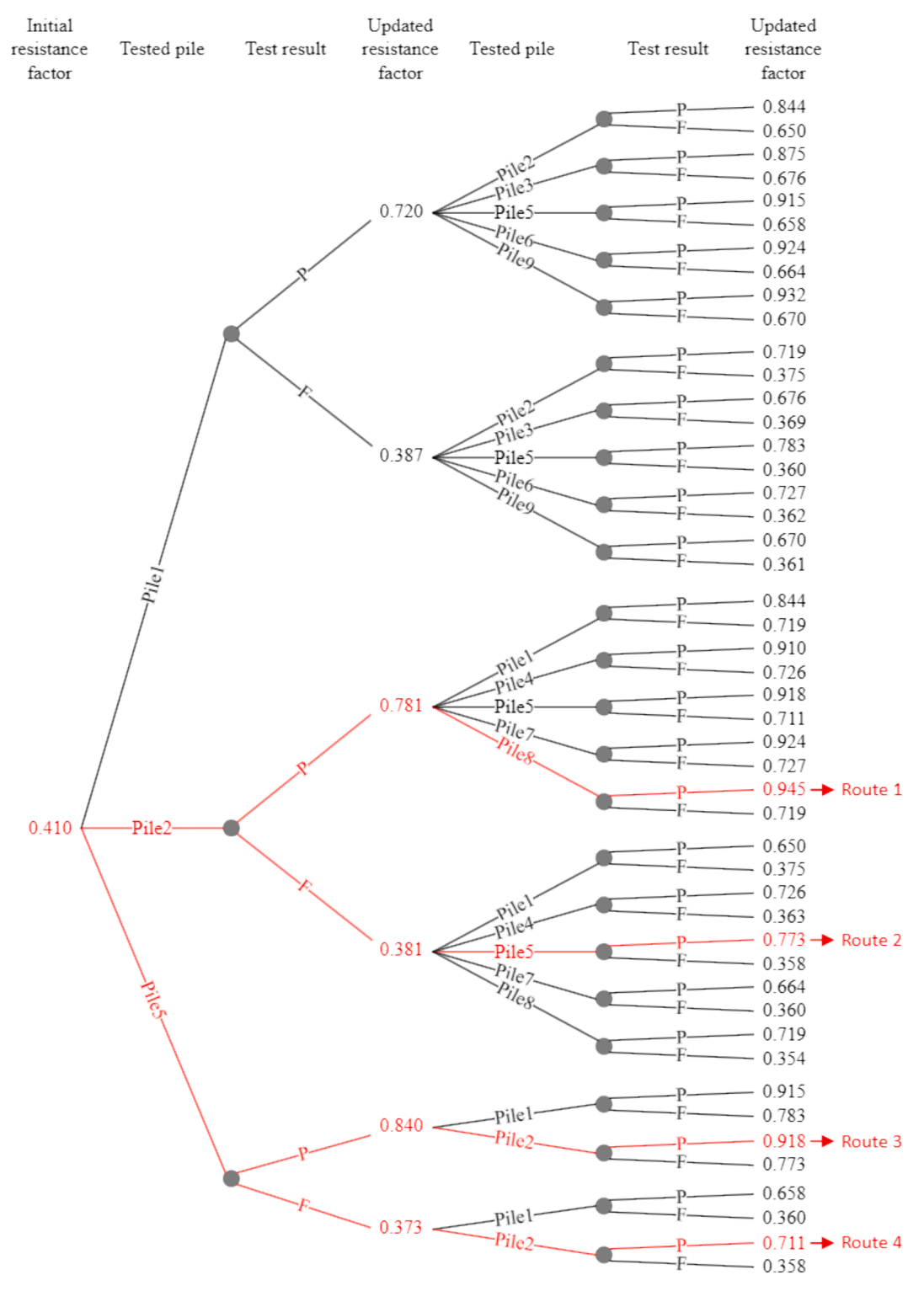


Fig. 7. Decision tree for selecting optimal test locations based on previous test results.

The observation indicates that the centre pile is the optimal test location when only one test is to be performed, while both centre and edge piles are viable choices for conducting the first load test if multiple tests are to be performed.

4. The proposed approach provides a systematic method to identify the optimal location for conducting subsequent load tests based on the obtained results. For instance, if the first load test is performed on the edge pile with a positive result, it is recommended to conduct the subsequent load test on the opposite edge pile. Conversely, if the first

load test is performed on the edge pile with a negative result, it is advised to conduct the next load test on the centre pile.

CRediT authorship contribution statement

Yuting Zhang: Conceptualization, Formal analysis, Methodology, Software, Validation, Writing – original draft. **Jinsong Huang:** Conceptualization, Funding acquisition, Methodology, Supervision, Validation, Writing – review & editing. **Jiawei Xie:** Methodology,

Validation, Writing – review & editing. Shan Huang: Methodology, Visualization, Writing – review & editing. Yankun Wang: Software, Writing – review & editing.

Declaration of competing interest

The authors declare that they have no known competing financial interests or personal relationships that could have appeared to influence the work reported in this paper.

Data availability

Data will be made available on request.

Acknowledgement

This work was supported by the National Natural Science Foundation of China (Project Nos. 41972280, 42272326). The first author wishes to acknowledge support from the China Scholarship Council (Grant No. 201906270257).

References

- Zhang Y, Huang J, Giacomini A. Bayesian updating on resistance factors of H-Piles with axial load tests. Comput Geotech 2023;159.
- [2] AS-2159-2009: Piling-Design and Installation. Standards Association of Australia; 2009.
- [3] Huang JS, Kelly R, Li DQ, Zhou CB, Sloan S. Updating reliability of single piles and pile groups by load tests. Comput Geotech 2016;73:221–30.
- [4] Park JH, Kim D, Chung CK. Implementation of Bayesian theory on LRFD of axially loaded driven piles. Comput Geotech 2012;42:73–80.
- [5] Zhang LM, Li DQ, Tang WH. Level of construction control and safety of driven piles. Soils Found 2006;46:415–25.
- [6] Zhang Y, Huang J. Calibration of resistance factor based on pile load test conducted to failure. In: 8th International symposium on geotechnical safety and risk (ISGSR). Newcastle (Australia): 2022.
- [7] Zhang L, Tang WH. Use of load tests for reducing pile length. Deep Foundations 2002: An International Perspective on Theory, Design, Construction, and Performance2002. p. 993-1005.
- [8] Zhang J, Li JP, Zhang LM, Huang HW. Calibrating cross-site variability for reliability-based design of pile foundations. Comput Geotech 2014;62:154–63.
- [9] Yang ZX, Jardine RJ, Guo WB, Chow F. A new and openly accessible database of tests on piles driven in sands. Geotechnique Letters 2015;5:12–20.
- [10] Tang C, Phoon KK. Statistics of model factors in reliability-based design of axially loaded driven piles in sand. Can Geotech J 2018;55:1592–610.
- [11] Eloseily KH, Ayyub BM, Patev R. Reliability assessment of pile groups in sands. Journal of Structural Engineering-Asce 2002;128:1346–53.
- [12] AbdelSalam SS, Sritharan S, Suleiman MT. LRFD resistance factors for design of driven H-piles in layered soils. J Bridg Eng 2011;16:739–48.
- [13] Paikowsky SG. NCHRP report 507: load and resistance factor design (LRFD) for deep foundations. Transp Res Board 2004.
- [14] Roling MJ, Sritharan S, Suleiman MT. Introduction to PILOT database and establishment of LRFD resistance factors for the construction control of driven steel H-piles. J Bridg Eng 2011;16:728–38.
- [15] Klammler H, McVay M, Herrera R, Lai P. Reliability based design of driven pile groups using combination of pile driving equations and high strain dynamic pile monitoring. Struct Saf 2013;45:10–7.
- [16] Becker DE. Eighteenth Canadian geotechnical colloquium: Limit states design for foundations. Part II. Development for the national building code of Canada. Can Geotech J 1997;33:984–1007.
- [17] Kwak K, Kim KJ, Huh J, Lee JH, Park JH. Reliability-based calibration of resistance factors for static bearing capacity of driven steel pipe piles. Can Geotech J 2010;47: 528–38
- [18] McVay MC, Birgisson B, Zhang LM, Perez A, Putcha S. Load and resistance factor design (LRFD) for driven piles using dynamic methods - A Florida perspective. Geotech Test J 2000;23:55–66.

- [19] Ng K, Sritharan S. Integration of construction control and pile setup into load and resistance factor design of piles. Soils Found 2014;54:197–208.
- [20] Ng KW, Sritharan S. A procedure for incorporating setup into load and resistance factor design of driven piles. Acta Geotech 2015;11:347–58.
- [21] Naghibi F, Fenton GA. Target geotechnical reliability for redundant foundation systems. Can Geotech J 2017;54:945–52.
- [22] Oudah F, El Naggar MH, Norlander G. Unified system reliability approach for single and group pile foundations - Theory and resistance factor calibration. Comput Geotech 2019;108:173–82.
- [23] Alhashmi AE, Oudah F, El Naggar MH. Application of binomial system-based reliability in optimizing resistance factor calibration of redundant pile groups. Comput Geotech 2021;129:103870.
- [24] Aashto. lrfd,. Bridge Design Specifications. 9th edition. American Association of State Highway and Transportation Officials; 2020.
- [25] Zhang LM, Tang WH, Ng CWW. Reliability of axially loaded driven pile groups. J Geotech Geoenviron Eng 2001;127:1051-60.
- [26] Poulos HG, Davis EH. Pile foundation analysis and design 1980.
- [27] Comodromos EM, Papadopoulou MC, Rentzeperis IK. Pile foundation analysis and design using experimental data and 3-D numerical analysis. Comput Geotech 2009; 36:819–36.
- [28] Poulos HG. Pile Behavior Theory and Application. Geotechnique 1989;39: 363–415
- [29] Allen TM. Development of new pile-driving formula and its calibration for load and resistance factor design. Transp Res Rec 2007;2004:20–7.
- [30] Meyerhof GG. Safety factors in soil mechanics. Can Geotech J 1970;7:349-55.
- [31] Tang WH, Woodford DL, Pelletier JH. Performance Reliability of Offshore Piles. All Days: Offshore Technology Conference; 1990.
- [32] Ching J, Phoon K-K. A quantile-based approach for calibrating reliability-based partial factors. Struct Saf 2011;33:275–85.
- [33] Ang A-H-S, Tang WHX. Probability concepts in engineering planning and design: Emphasis on application to civil and environmental engineering. Hoboken, New Jersey: Wiley; 2007.
- [34] Haario H, Laine M, Mira A, Saksman EDRAM. Efficient adaptive MCMC. Stat Comput 2006;16:339–54.
- [35] Naghibi M, Fenton GA. Geotechnical resistance factors for ultimate limit state design of deep foundations in cohesive soils. Can Geotech J 2011;48:1729–41.
- [36] Ronold KO. Characteristic soil strength for axial pile capacity and its estimation with confidence for offshore applications. Struct Saf 2016;63:81–9.
- $[37] \ \ Itasca\ Consulting\ Group\ I.\ FLAC3D\ -- \ Fast\ Lagrangian\ Analysis\ of\ Continua\ in\ Three-Dimensions,\ Ver.\ 6.0.\ Minneapolis:\ Itasca2017.$
- [38] Issmfe. Axial Pile Loading Test—Part 1: Static Loading. Geotech Test J 1985;8: 79–90.
- [39] Zhang LM, Li DQ, Tang WH. Reliability of bored pile foundations considering bias in failure criteria. Can Geotech J 2005;42:1086–93.
- [40] Leung YF, Lo MK. Probabilistic assessment of pile group response considering superstructure stiffness and three-dimensional soil spatial variability. Comput Geotech 2018:103:193–200.
- [41] Li Y, Fenton GA, Hicks MA, Xu N. Probabilistic Bearing Capacity Prediction of Square Footings on 3D Spatially Varying Cohesive Soils. J Geotech Geoenviron Eng 2021:147.
- [42] Johari A, Talebi A. Stochastic Analysis of Piled-Raft Foundations Using the Random Finite-Element Method. Int J Geomech 2021;21.
- [43] Kong L, Zhang L. Lateral or torsional failure modes in vertically loaded defective pile groups. GeoSupport 2004: Drilled shafts, micropiling, deep mixing, remedial methods, and specialty foundation systems2004. p. 625-36.
- [44] Zhang Q-q, Zhang Z-m. Simplified calculation approach for settlement of single pile and pile groups. J Comput Civ Eng 2012;26:750–8.
- [45] Haldar S, Babu GLS. Response of vertically loaded pile in clay: a probabilistic study. Geotech Geol Eng 2012;30:187–96.
- [46] Griffiths DV, Fenton GA, Manoharan N. Bearing capacity of rough rigid strip footing on cohesive soil: probabilistic study. J Geotech Geoenviron Eng 2002;128: 743–55.
- [47] Heße F, Prykhodko V, Schlüter S, Attinger S. Generating random fields with a truncated power-law variogram: A comparison of several numerical methods. Environ Model Softw 2014;55:32–48.
- [48] Crisp MP, Jaksa MB, Kuo YL. Characterising site investigation performance in multiple-layer soils and soil lenses. Georisk-Assessment and Management of Risk for Engineered Systems and Geohazards 2021;15:196–208.
- [49] Naghibi F, Fenton GA. Design of foundations against differential settlement. Can Geotech J 2022;59:384–96.
- [50] Zhang X-I, Jiao B-h, Han Y, Chen S-I, Li X-y. Random field model of soil parameters and the application in reliability analysis of laterally loaded pile. Soil Dyn Earthq Eng 2021;147:106821.